

# RELIABLE LABEL EFFICIENT LEARNING OF EEG ACQUISITION USING ELECTRODES

Mrs.P.Jegadeeshwari  
Department of ECE

CK College of Engineering and Technology,  
Cuddalore, Tamil Nadu, India

Mrs.R.Nithya  
Department of ECE

CK College of Engineering and Technology,  
Cuddalore, Tamil Nadu, India

**Abstract**— Active Electrodes with in built read out circuitry in progressive increase are being executed in wearable healthcare and lifestyle applications due to AE's robustness to environmental interference. An AE locally amplifies and buffers  $\mu\text{V}$ -level EEG signals before driving any cabling. The low output impedance of an AE alleviate cable motion artifacts thus enabling the use of high-impedance dry electrodes for greater user comfort. However, developing a wearable EEG system, with medical grade signal quality on noise, electrode offset tolerance, common-mode rejection ratio (CMRR), input impedance and power dissipation, remains a challenging task. This paper reviews state-of-the-art bio-amplifier architectures and low-power analog circuits design techniques intended for wearable EEG acquisition, with a special focus on AE system interfaced with dry electrodes.

**Index Terms**—Active electrode, instrumentation amplifier (IA), electroencephalography (EEG), dry electrodes, common-mode rejection ratio (CMRR), brain-computer interface (BCI)

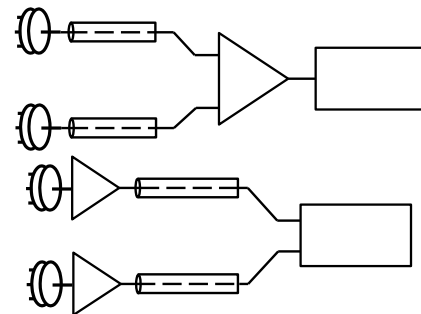
## I. INTRODUCTION

Today, miniature and low-power medical sensors can be easily integrated into various accessories that continuously sense, process and transfer people's physiological information during their daily life activities. By reducing the need for manual intervention and by lowering the cost, these medical devices are being widely used in personal healthcare and home diagnostics, such as wellness and health monitoring, home rehabilitation, and the early detection of brain disorders [1][2].

Electroencephalography (EEG) is one of the most important methods to monitor the electrical behaviors of the brain and to evaluate brain disorders. In recent years, the growing need for continuous and comfortable brain activities monitoring have promoted the development of wearable EEG devices for both clinical and non-clinical applications [3]-[5], from deep sleep monitoring, epileptic seizure detection, mental state analysis, to Dry electrodes solve this problem by eliminating the need for gel, which in turn enables a faster setup time and greater user comfort, but the tradeoff is electrode-skin impedance.

Recent advances in biomedical technologies, integrated circuits (ICs), sensors and data analysis techniques have gaming, sports, and military use. However, a remaining

issue of standard EEG devices is their dependence on gel electrodes, e.g. wet electrodes, which can improve reliability and signal integrity at the expense of inconvenience and discomfort. Moreover, gel will eventually dry out, resulting in degraded recording quality and the need for electrode replacement. These drawbacks prevent wet electrodes being used for long-term and continuous EEG monitoring, especially when a large number of electrodes are placed on scalp.



An electrode with a co-integrated amplifier (Fig. 1), i.e. an *Active Electrode (AE)*, reduces noise pickup by minimizing the routing between the electrode and the amplifier. Furthermore, the amplifier's low output impedance mitigates cable motion artifacts, thus eliminating the use of shielded cables for low cost [7]. On the other hand, an AE based system typically require more wires (e.g. power supply and reference) compared to a conventional EEG readout circuitry, especially when additional functions (e.g. impedance measurement) are integrated in AEs.

## II. ELECTRODE-TISSUE INTERFACE

Biopotential electrodes convert ionic physiological signals to electrical signals. As the first component of signal acquisition chain, the characteristics of electrode-tissue interface can be a system performance limiting factor. Practical concerns for electrodes are materials, polarization voltage, electrode-tissue impedance (Fig. 2), and user comfort. The concepts and materials of biopotential electrodes highly depend on their applications. Body surface electrodes for wearables can be grouped into the following categories [8]: metal-plate



electrodes (long-term), disposable foam-pad electrodes (low cost), metallic suction electrodes (no strap), floating electrodes (minimize motion artifacts), flexible electrode (comfortable), and internal needle electrode (subdermal). For wearable scalp EEG measurement, flexible metal/polymer electrodes with pins sliding through hair are the most popular form factors for high-quality scalp contact. The concepts and materials of biopotential electrodes highly depend on their applications.

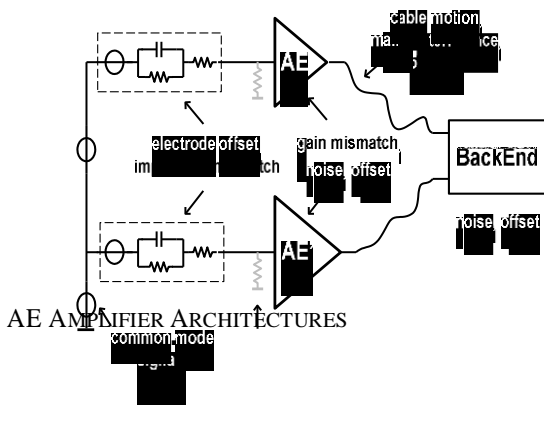
Body surface electrodes for wearables can be grouped into the following categories [8]: metal-plate electrodes (long-term), disposable foam-pad electrodes (low cost), metallic suction electrodes (no strap), floating electrodes (minimize motion artifacts), flexible electrode (comfortable), and internal needle electrode (subdermal). For wearable scalp EEG measurement, flexible metal/polymer electrodes with pins sliding through hair are the most popular form factors for high-quality scalp contact. Regarding to the electrode materials, gold (Au), platinum, silver chloride (AgCl) and sintered Ag/AgCl are common used. Gold and platinum electrodes are expensive, but are robust and easy to maintain.

### III. PERFORMANCE CRITERIA OF AE READOUT CIRCUITRY

AE-based wearable EEG systems should be designed to meet the following requirements compliant with medical standards, which impose constraints on the electrical performance of an AE system in terms of its noise, input impedance, electrode offset tolerance, common-mode rejection ratio (CMRR), power dissipation etc. (Table I). The following sections will discuss major specifications and challenges in detail.

#### Noise

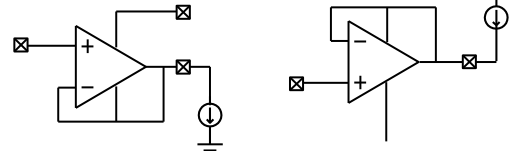
According to the IEC standard [19], an EEG system should exhibit the maximum input-referred noise of  $6\mu\text{V}_{pp}$  to detect  $\mu\text{V}$ -level EEG signals. This nominal peak-to-peak noise can be converted to the root mean square (rms) noise by dividing a factor of 6.6 [22], resulting in an integrated noise of  $0.91\mu\text{V}_{rms}$ . As a result, state-of-the-art bio-amplifiers usually target for an input-referred noise of  $<1\mu\text{V}_{rms}$  in a 0.5Hz to 100Hz bandwidth. Furthermore, their  $1/f$  noise is typically mitigated by dynamic circuit techniques (see section V.B).



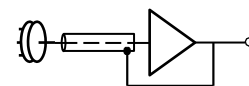
In an AE-based EEG system, the choice of either a buffer or an *instrumentation amplifier (IA)* is an important architectural decision. This is because the selected architecture has a major impact on the system specifications, e.g. input dynamic range, power budget, noise performance, cabling requirements, etc.

#### Analog Buffers

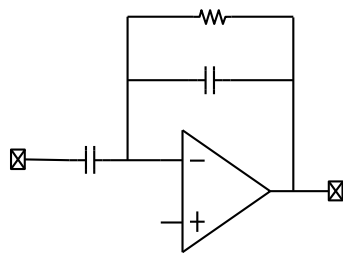
An analog buffer, i.e. a voltage follower, is the most popular architecture as an AE because of balanced analog performance, e.g. high input impedance, low output impedance and low gain variation. Furthermore, a buffer only requires 3 wires ( $V_{dd}$ ,  $V_{ss}$  and  $V_{out}$ ) connected to a backend processor. Novel buffers have been invented towards higher input impedance and fewer wires. In [23], ultra-high input impedance ( $60\text{fF}/5\text{T}\Omega$ ) is achieved via using an impedance bootstrapping technique. In [24], an output current driver enables the buffer's analog output to be shared with negative supply via a single wire, at the cost of  $1/2$  output dynamic range (Fig. 4a). A similar principle is presented in [25], where the analog output is combined with the buffer's positive supply; however, to maintain a large output dynamic range, the buffer is powered by a 5V supply voltage (Fig. 4b).



An analog buffer also facilitates the use of active shielding [26], a well-known technique to reduce the interference coupled to the inner lead wire. Active shielding is realized by driving a shield mesh wrapped around the inner lead wire to insulate biopotential signals from the external interference. The driving signal which is fed back to the shield mesh should be the same as input biopotential signal but in a low-impedance manner. An analog buffer is an ideal solution for low-power active shielding, because its low-impedance output can drive the shield mesh directly.



AC-coupled inverting amplifiers with capacitive feedback [27] address both issues, thus being widely used in wearable and implantable medical instruments [28][29]. An AE built with a capacitively coupled inverting amplifier [30] is shown in Fig. 6. This AE exhibits balanced analog performance, e.g. low noise of  $0.8\mu\text{V}_{rms}$ , rail-to-rail electrode offset tolerance, low power dissipation of  $20\mu\text{W}$ . To realize a cutoff frequency  $<0.5\text{Hz}$ , a large resistor of a few tens of  $\text{G}\Omega$  is required. To avoid the need for an external component, an on-chip pseudo-resistor [27] was implemented (see Section III.C), at the cost of nonlinearity and inaccuracy of the resistance.



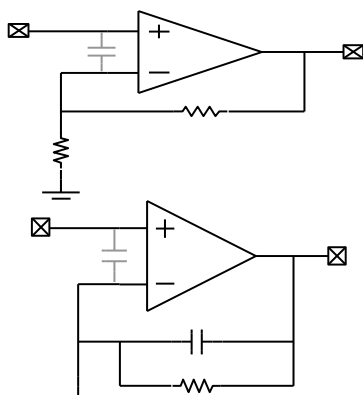
The power of a capacitively coupled inverting amplifier can be further reduced by optimizing its core amplifier [31]-[33]. Apart from the general guidelines of low-power amplifiers (see Section V.A), a state-of-the-art bio-amplifier [34] achieves low noise of  $0.34\mu\text{V}_{\text{rms}}$  with only  $1.17\mu\text{W}$  power, corresponding to a noise-efficiency-factor (NEF) of 1.74. Such a power-efficient design is realized by combining a localized low supply voltage of 0.6V together with an inverter-based current reuse technique

A remaining challenge of a capacitively coupled amplifier is its parameter tradeoff between input impedance and noise [35], both are related to the input coupling capacitor  $C_1$ .

#### Non-Inverting Amplifiers

Non-inverting amplifiers have higher input impedance than inverting amplifiers, so AEs implemented with non-inverting amplifiers using resistive feedback (Fig. 7a) were proposed in [36][37]. The input resistor ( $R_i$ ) is a primary noise contributor, and so it is typically in the order of a few k $\Omega$ . However, such a low resistance then increases the amplifier's load and power dissipation.

Alternatively, non-inverting amplifiers can utilize capacitive feedback [38] (Fig. 7b) to mitigate resistor noise. This amplifier architecture can tolerate  $\pm 300\text{mV}$  electrode offset because their DC gain are always unity regardless of AC gain. The residual offset can be compensated with the help of a so-called DC servo loop (DSL), which tracks and attempts to null the output offset by negative feedback (see Section V.C)

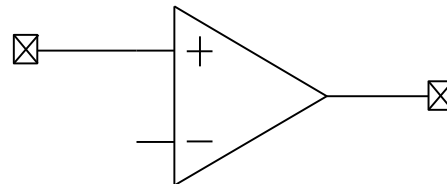


*DC-Coupled Amplifiers*

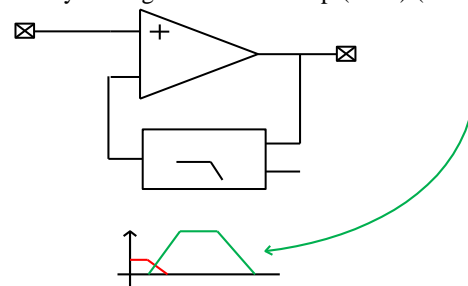
The AC-coupled amplifiers described above not only reject electrode offset, but also block very low frequency signals and induce distortion. AC-coupled amplifiers can therefore not be used to measure slow cortical potentials (SCP) [39],

where extremely low frequency ( $<1\text{Hz}$ ) surface voltage is monitored for various cognitive tasks (e.g., language) and sensory-motor tasks (e.g., motor preparation and expectation) [40].

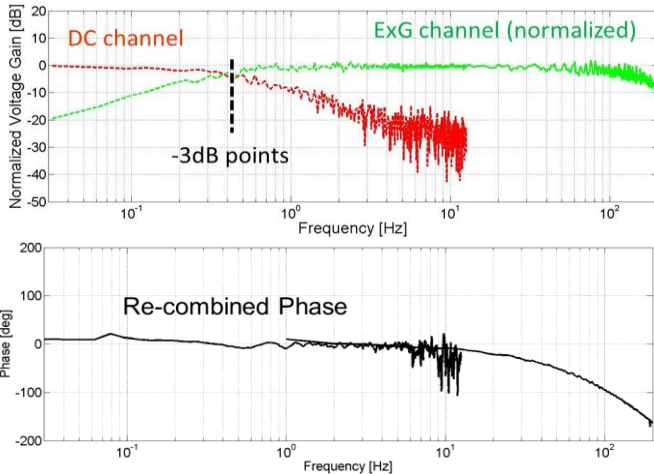
A DC-coupled amplifier (Fig. 8) would preserve these low frequency signals, but its gain would be limited by a large dynamic range ( $>90\text{dB}$ ) determined by electrode offset and  $\mu\text{V}$  EEG signals. In addition, A high-resolution ADC ( $>16$  bit) is typically required to meet the noise specifications [41], leading to significant power dissipation in a multi-channel system [42].



A DC-coupled amplifier can be realized with many different architectures, e.g. current balancing amplifiers [43][44], current feedback amplifiers [45][46], three-opamp amplifiers [47], and capacitively coupled chopper amplifiers [35][48]. In case DC measurement is not mandatory, a DC-coupled amplifier can be easily converted into an AC-coupled amplifier by adding a DC servo loop (DSL) (see section V.C).



An alternative DC-coupled amplifier, namely “functionally” DC-coupled amplifier [49][50], can combine the advantages of both AC-coupled and DC-coupled amplifiers, i.e. very large electrode offsets tolerance ( $\pm 350\text{mV}$ ) at low power ( $<1\mu\text{W}$ ) while still remaining DC-coupled. This is accomplished by utilizing a DC-servo loop based on voltage-to-voltage feedback (Fig. 9), which tracks the offset at the amplifier's output and cancels it by driving the inverting input of the amplifier. As a result, the AC-coupled EEG signals are available at the amplifier's output, while the DC and extremely low frequency signals are available at the output of the DC-servo loop with unity gain.



Although the DC servo loops can also be implemented with a voltage-to-current feedback [35][43][48], however, this suffers from a performance tradeoff between electrode offset tolerance and power (see section V.C), which limits the offset tolerance to roughly 50mV.

#### IV. CIRCUIT DESIGN TECHNIQUES

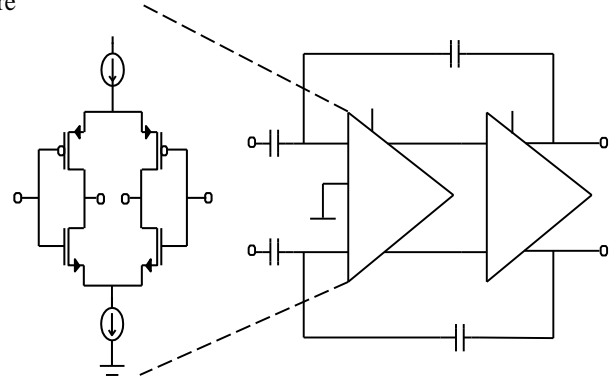
Although numerous amplifier architectures have been used as AEs, they all involve various performance tradeoffs and so no ideal architecture has yet emerged. Zooming in from system level to circuit level, this section reviews various circuit design techniques to improve the AE-specific specifications listed in section III.

##### Power Reduction

At the system level, a major drawback of a buffer-based AE system is its low noise-to-power efficiency. A low-noise buffer is power hungry, and it only performs impedance conversion without providing any voltage gain. As a result, the next stage (Fig. 3) has to overcome the same challenges of noise and electrode offset tolerance, reducing system's power efficiency. Alternatively, to improve the noise-to-power efficiency, an AE can be implemented as an instrumentation amplifier, of which the voltage gain relaxes the noise requirement of the succeeding stage [30]. However, using two amplifiers (as one EEG channel) poses a different challenge in terms of CMRR degradation due to their gain mismatch.

At the circuit level, the AE's noise specification drives the overall power budget. A conventional amplifier has to increase the amount of power to reduce the thermal noise. However, novel circuit techniques can achieve the same target with low power. Current reuse [33], e.g. by using an inverter-based input transistors consisting of series-connected NMOS and PMOS (Fig. 11), doubles the input transconductance without adding any tail current, but at the expense of  $\frac{1}{2}$  input dynamic range. State-of-the-art

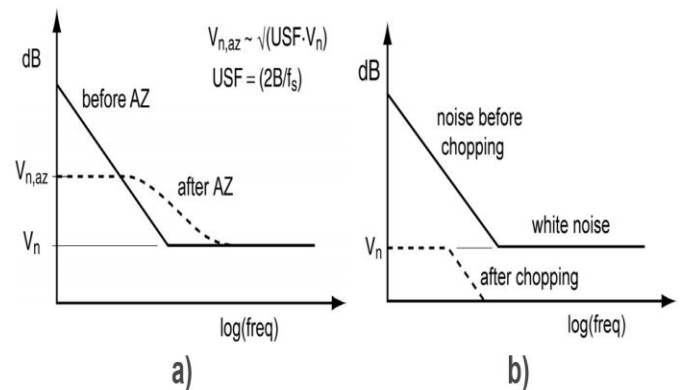
capacitively coupled bio-amplifiers employing similar techniques achieve low noise-efficient factors (NEFs) of 1.74 [34] and 2.1 [51] by further reducing the supply voltage of the first stage (Fig. 11). Both designs exploit the fact that the amplifier's inputs ( $v_n$ ,  $v_p$ ) are at virtual ground and so the core



##### Noise Reduction

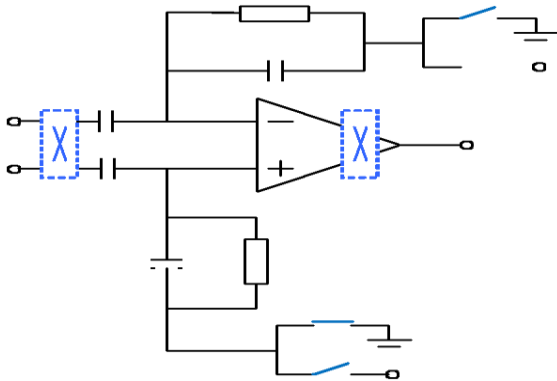
Apart from thermal noise,  $1/f$  noise (flicker noise) is usually the dominant noise source of a bio-amplifier because the noise bandwidth can be a few kHz. Conventionally,  $1/f$  noise can be reduced by enlarging the size of the input transistors, but using extremely large transistors not only takes up more space but also reduces input impedance by adding parasitic capacitances.

Alternatively, dynamic circuit techniques can mitigate the amplifier's  $1/f$  noise and intrinsic offset in a power- and area-efficient manner. Two well-known dynamic techniques include auto-zeroing (AZ) and chopping (Fig. 12) [52]. AZ operates in two phases. Noise and offset are sampled and stored in the first phase, and so they will be compensated in the second phase. Drawback of AZ is that high frequency noise is folded back and distributed over the bandwidth of  $f_s/2$  (Fig. 13a). Chopping operates continuously by periodically swapping the amplifier's inputs, which modulates the  $1/f$  noise and offset to a chopping frequency  $f_c$ , thus no noise folding exists (Fig. 13b).



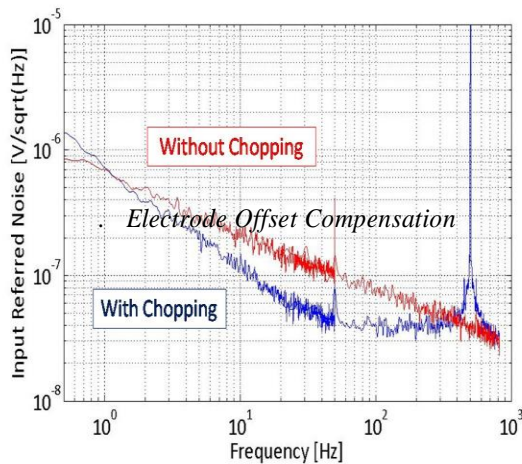


CHOPPERS HAVE BEEN IMPLEMENTED AT DIFFERENT LOCATIONS OF AN AMPLIFIER. FOR EXAMPLE, IN A CAPACITIVELY COUPLED AMPLIFIER, AN INPUT CHOPPER CAN BE PLACED BEFORE THE INPUT COUPLING CAPACITOR [35][48] (FIG. 14A). HOWEVER, THIS CHOPPER SCHEME EFFECTIVELY REALIZES A DC-COUPLED AMPLIFIER, WHICH HAS A LIMITED ELECTRODE OFFSET TOLERANCE OF ONLY A FEW TENS OF MV.



On the other hand, the input chopper can be placed inside the feedback loop [30][54], i.e. at the amplifier's virtual ground (Fig. 14b). This chopper scheme ensures rail-to-rail electrode offset tolerance, but it suffers from  $1/f^2$  noise (Fig. 15) due to chopper-induced current noise at a high impedance node [55].

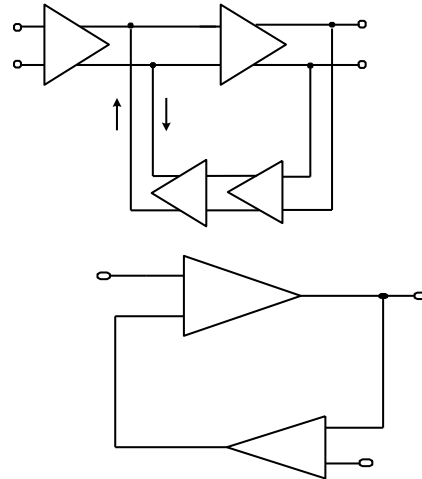
The  $1/f^2$  noise has been observed in other chopper amplifier architectures, such as a non-inverting chopper amplifier [38], inverting chopper amplifiers [30][56], and a chopper amplifier equipped with an external floating high-pass filter (HPF) [44]. The common problem of these amplifiers is that chopping was always performed at very high-impedance node (in  $G\Omega$  range).



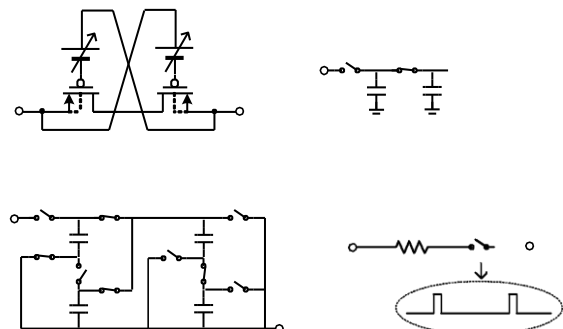
AC-coupling via capacitor is the most obvious way to enable electrode offset rejection. However, large capacitors of at least a few tens of pF hinder area efficiency. A DC-servo loop (DSL), i.e. a feedback loop with low-pass filter ( $<0.5\text{Hz}$ ) characteristic, can compensate electrode offset as well. A DC-

servo loop can be implemented via either a current feedback (Fig. 16a), or a voltage feedback (Fig. 16b).

IN CURRENT FEEDBACK DSLs [35][43][48], THE MAXIMUM OFFSET TOLERANCE IS USUALLY LIMITED ( $<50\text{mV}$ ), IT SUBJECTS TO THE AMOUNT OF COMPENSATION CURRENTS ( $I_{DC}$ ) AND POWER.



A common challenge of a DSL is to implement a sub-Hertz cutoff frequency. State-of-the-art amplifiers emulate an on-chip  $G\Omega$ -range resistor as follows (Fig. 17): a pseudo-resistor [27], a switched-capacitor (SC) resistor [35], and a switched-resistor resistor [57].



A DSL can also be implemented with calibration for coarse offset compensation, where a digital-to-analog converter (DAC) periodically compensates electrode offset with digital codes as input. The digital codes controlling the DAC can be generated differently. In [60], a coarse offset compensation was presented, where the amplifier's output baseline is regulated between two predefined threshold voltages by using a current steer DAC to avoid hard clipping. In [30], the input offset of the amplifier is mostly compensated by a foreground calibration. The current steering DAC, controlled by successive approximation register (SAR) logics, calibrates the offset from



220mV to 20mV in 7 clock cycles. In general, calibrating the offset has the advantage of being low power, since it is only active before the signal.

## V. REFERENCES

- [1] S. Patel, H. Park, P. Bonato, L. Chan, and M. Rodgers, "A review of wearable sensors and systems with application in rehabilitation," *IEEE Journal of Neuro Eng. and Rehabilitation*, vol. 9, pp. 21, Jan. 2012.
- [2] X.-F. Teng, Y.-T. Zhang, et al., "Wearable Medical Systems for p-Health" *IEEE Reviews in Biomedical Engineering*, vol.1, pp.62-74, Dec. 2008.
- [3] B. Gyselinckx, C. Van Hoof, et al., "Human++: Autonomous wireless sensors for body area networks," *Proc. Custom Integrated Circuit Conf (CICC)*, pp.13-19, Sept. 2005.
- [4] M.A. Lopez-Gordo, et al., "Dry EEG electrodes," *Sensors*, vol. 14, no. 7, pp. 12847-12870, 2014.
- [5] M. De Vos, S. Debener, "Mobile EEG: towards brain activity monitoring during natural action and cognition," *Int. J. Psychophysiol.*, vol. 91, no. 1, pp. 1-2, 2014.
- [6] Y. M. Chi, T.-P. Jung, and G. Cauwenberghs., "Dry-contact and noncontact biopotential electrodes: methodological review," *IEEE Reviews in Biomedical Engineering*, pp.106-119, Dec. 2010.
- [7] A. C. Metting-van Rijn, et al., "Low cost active electrode improves the resolution in biopotential recordings," *Proc. IEEE Eng. Med. Bio. Conf.*, pp. 101-102, 1996.
- [8] M. R. Neuman, "Biopotential Electrodes." *The Biomedical Engineering Handbook: Second Edition*. CRC Press LLC, 2000.
- [9] P. Tallgren, et al., "Evaluation of commercially available electrodes and gels for recording of slow EEG potentials," *Clin Neurophysiol.* vol. 116, no. 4, pp. 799-806, April. 2005.
- [10] D. Henrich, et al., "New Dry Electrodes with Comparable Performance as Standard Electrodes," *Biomedical Engineering*, issue. 58, Sept. 2013.
- [11] R. Dozio, A. Baba, et al., "Time based measurement of the impedance of the skin-electrode interface for dry electrode ECG recording," *Proc. IEEE Eng. Med. Biol. Soc. Conf.*, pp. 5001-5004, Aug. 2007.
- [12] A. R. Motaa, et al., "Development of a quasi-dry electrode for EEG recording," *Sensors and Actuators A*, vol.199, pp. 310-317, Sept. 2013.
- [13] S. Lee and J. Kruse, "Biopotential electrode sensors in ECG/EEG/EMG systems", *Analog Devices*, 2008.
- [14] C. Grozea, C. D. Voinescu, et. al., "Bristle-sensors-Low-cost Flexible Passive Dry EEG Electrodes for Neurofeedback and BCI Applications," *IEEE J. Neural Eng.*, pp.1-14, Mar. 2011.
- [15] C. T. Lin, L. D. Liao, et al., "Novel Dry Polymer Foam Electrodes for Long-Term EEG Measurement," *IEEE Trans. on Biomed. Engineering*, vol. 58, issue. 5, pp.1200-1207, Dec. 2010.
- [16] S.M. Lee, et al., "A capacitive, biocompatible and adhesive electrode for long-term and cap-free monitoring of EEG signals," *J. Neural Eng.*, vol.10, 036006, Apr. 2013.